SLAC–PUB–5404
December 1990
(I)

STUDY OF HADRONIC AND ELECTROMAGNETIC SHOWER DEVELOPMENT BETWEEN 10 AND 140 GEV BY AN IRON-SCINTILLATOR CALORIMETER*

EMLYN HUGHES
Stanford Linear Accelerator Center
Stanford University, Stanford, CA 94309

ABSTRACT

Results are presented on the analysis of CDHS test beam data using an iron-scintillator calorimeter exposed to electrons and pions in the energy range 10 to 140 GeV. Shower development is studied in order to extract information on calorimetric response to electrons and pions, longitudinal and transverse shower profiles, shower containment and correlations, muon punch through and the effect on energy resolutions due to dead materials.

Introduction

In order to study shower simulations and to design large scale detectors for future colliders, data on shower development with high energies beams and with simple and large calorimeters are invaluable. This report provides the results of a study using test beam data with an iron-scintillator calorimeter from the CDHS detector at CERN. The data represents measurements of electron and pion induced interactions in test beam runs in 1982 and 1984.

The report is organized into two parts. The first part describes the experimental set up with details on the beam and the calorimeter. The second part gives the results of the data analysis. The second section begins with a discussion of calibration and event selection. Results are presented on the measurement of the interaction length, the ratio of the response to electrons versus pions and electrons versus muons, longitudinal and transverse shower development, shower containment, shower correlations, muon punch through and studies of the effect of dead materials on the energy response and resolution.

Compared to previous calibration runs of the CDHS detector,[1] the present data has the advantage of presenting high statistics pion data down to energies of 10 GeV and a collimated electron beam with energies up to 140 GeV. The present data also uses the upgraded version of the CDHS calorimeter, which have finer transverse and longitudinal shower sampling.

*Work supported by Department of Energy contract DE–AC03–76SF00515.

Invited talk presented at the International Conference on Calorimeters in High Energy Physics, October 29–November 1, 1990

Experimental Setup

Test Beam

The test beams analyzed in this report were generated by protons produced in the CERN SPS impinging on a Beryllium target. Secondary pions and electrons were selected with specific momentum in a beam line downstream of the target. A 5 mm lead absorber was placed upstream in the beam line in order to remove secondary particles for the pion runs. For the electron beam, a sweeping magnet placed directly after the target dispersed all charged particles out of the beam line. Electrons from photon conversion were subsequently tagged by two helium threshold Cerenkov counters run in coincidence up to energies of 50 GeV. Electron and pion beams were run separately at energies of 10, 15, 20, 30, 50, 75, 100, 120 and 140 GeV.

The data presented in this report comes from two separate test beam runs, both used for calibrating the CDHS detector for its neutrino physics program at CERN. The S3 test beam was used in 1982 and the X5 test beam was used in 1984. After cuts, 4000 to 13000 events per beam energy existed for the pion data in 1982 as opposed to 1000 to 3000 in 1984. But only the 1984 test run provided electron data with 1000 to 3200 events accepted per beam energy. Measurements of the detector's energy resolution only exists for the 1982 data, since the beam had a momentum spread of less than 1%. The momentum spread of the 1984 X5 test beam was between 5 and 10%. The average beam energy for the 1984 data was known to $\pm$ 0.5%.

Calorimeter

The calorimeter consisted of sixteen planes from an upgraded version of the CERN-Dortmund-Heidelberg-Saclay-Warsaw (CDHS) detector. Each plane contained five 25 mm thick iron plates (figure 1). Between these plates are sandwiched layers of scintillator strips with each group of five scintillators feeding into a plexiglass light guide which is viewed by a single 3 inch photomultiplier. Per plane there are 48 scintillators (24 left, 24 right), each 15 cm wide. Scintillators in adjacent planes alternate between horizontal and vertical. This configuration manifests itself in a lateral shower position resolution of $\sim$ 5 cm. Data collection occurred within a 2 second spill gate in which typically 5 to 40 events were accepted per burst. Only particles passing through an 8×8 strip hodoscope placed directly in front of the calorimeter were triggered upon. Each scintillator in the hodoscope was 5 cm wide. The calorimeter trigger required more than 3 GeV energy deposition in the apparatus, the same condition as in the neutrino scattering experiments.

Calibration and Results

Event Calibration and Selection

The calibration of the scintillator planes was done using cosmic muon data selected with the help of drift chambers placed between each four planes. The pulse height deposited by these cosmic muons was measured using the signal from photomultipliers amplified by 30 dB. The truncated average pulse height of these cosmic muons monitored the sensitivity of each photomultiplier. A measurement of the sensitivities of the photomultipliers with cosmic events showed a change of less than 1% on average over a two day period.

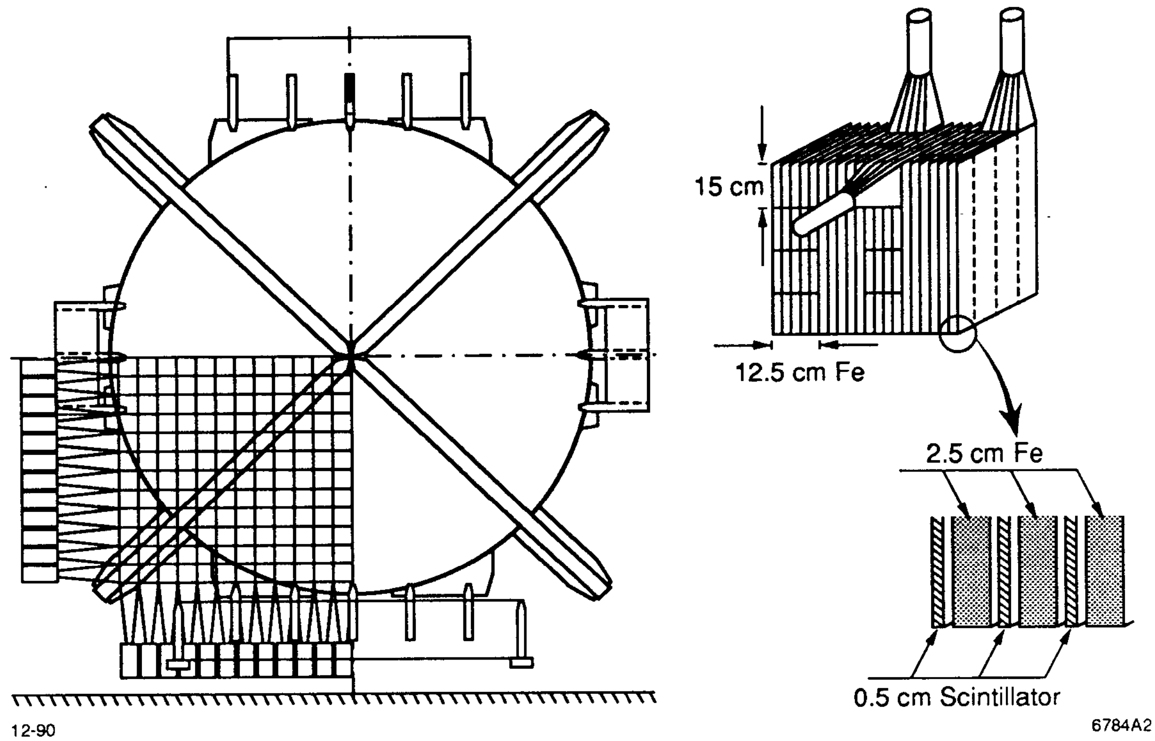

Fig. 1. Schematic view of the CDHS calorimeter. Five scintillators are viewed by one photomultiplier per plane. Each plane spans 12.5 cm of iron. Scintillator fingers alternate between horizontal and vertical per plane.

The charge deposited by a cosmic muon traveling through one plane (12.5 cm iron) of the calorimeter parallel to the axis provided the basic calibration unit: Number of Equivalent Particles (NEP). Measurements of the shower energy deposited in the calorimeter are, throughout this report, expressed in NEPs.

Events were selected with the following criteria:

- The particles had to pass through the central four bins of the hodoscope (10×10 cm).
- No hit in any scintillator further than 75 cm from the hodoscope center was allowed in the first two planes of the calorimeter. This condition eliminated contamination from upstream interactions.
- Events whose longitudinal shower energy distribution was long and flat were rejected in order to remove incoming muons.

In each study the minimum accepted scintillator response was 0.3 NEP. Varying this cut to 0.6 NEP changed the average energy response by less than 1% at 140 GeV and by 2% at 10 GeV for pion induced interactions.

Interaction Length Measurement

To find the interaction length of the pion induced showers, a vertex for each event was identified. The vertex was chosen to be the first plane in which the amount of energy deposited exceeded 3 NEP. A plot of the vertex position as a function of depth is given in figure 2. The fall off is exponential and a fit to the distribution gives the interaction length. The interaction length was found to be 19 ± 1 cm for 10 GeV showers and 20 ± 1 cm for 140 GeV showers. The uncertainty comes from the fit. The present interaction length measurement agrees with the previous CDHS result.[1]

The measurement depends somewhat on the minimum vertex energy definition, namely the amount of energy deposited in the first plane as long as the first plane energy cut is high. Figure 3 shows the interaction length measurement as a function of the minimum energy cut which defined the vertex plane. Figure 3 shows clearly that when the energy cut for the vertex is too low, the ionization energy deposited by the incoming pions gives a vertex definition which is upstream of the true interaction vertex.

Response to electrons versus pions

The primary motivation for these test beams was to calibrate the CDHS detector for neutrino interactions. In these tests, the energy response and resolution of the detector were measured and corrected for fluctuations.[1] In this paper no corrections are implemented. Only the sum over the raw NEP response is given for the total shower energy measurement. Figure 4 shows an example of a typical shower energy distribution for a 50 GeV pion beam. A Gaussian fit to the distribution is done for each energy. The results of the average energy (peak value) and resolution (width) are given in table 1.

A measurement of the electron versus pion response yields about a 20% difference between average energy deposited as shown in figure 5.

Response to electrons and muons

A discussion of whether calorimetric response to electrons and muons is identical was raised in a previous calorimeter conference.[2] A comparison between the energy response of electrons and muons is done using the test beam data to determine the electron response and using muons from charged current neutrino interactions to determine the muon response.

In the last run of the CDHS detector,[3] an extensive study of the energy loss of muons from charged current neutrino interactions was done. The result of this study found that an average charged current muon would deposit 12.4 ± 0.2 NEP of energy as it traversed 1.5 meters of iron. The average momentum of these muons determined by a fit to the curvature of the track in a magnetic field was 7.8 ± 1.4 GeV. Using the measurements of dE/dx for muons,[4] the average energy lost by the muons in the 1.5 meters of iron was 2.65 ± 0.04 GeV where the error is a consequence of the uncertainty in the average muon momentum. Comparing the measured energy deposited with the energy loss expected gives a ratio of NEP/GeV $= 4.7 \pm 0.1$ for the response to muons in the calorimeter.

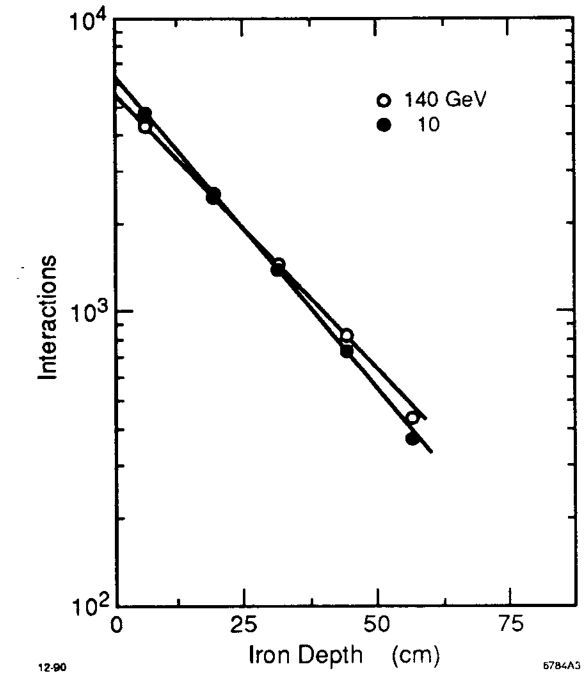

Fig. 2. Number of events as a function of the depth of the vertex in iron. Vertex plane is defined as the first plane in the shower with an energy greater than 3 NEP. Results are given for 10 and 140 GeV pion beams.

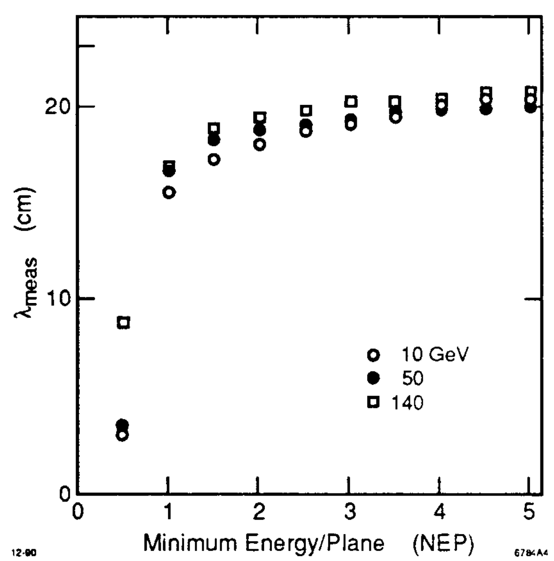

Fig. 3. Interaction length measurement as a function of energy cut for vertex definition.

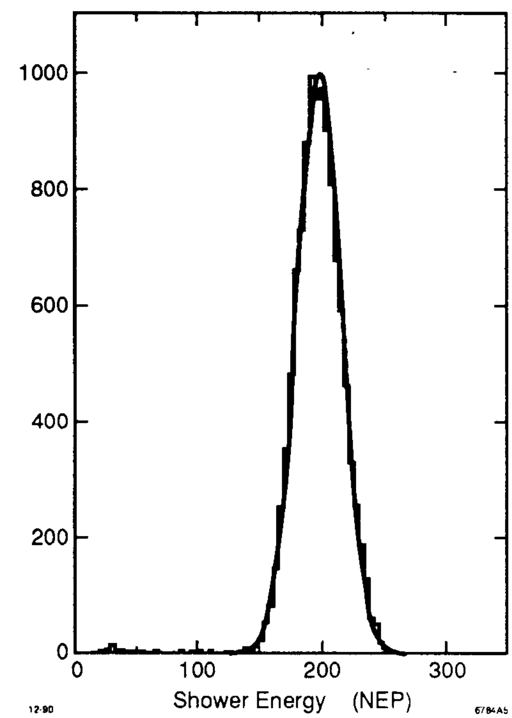

Fig. 4. Shower energy distribution for 50 GeV pions. Units are given in NEP.

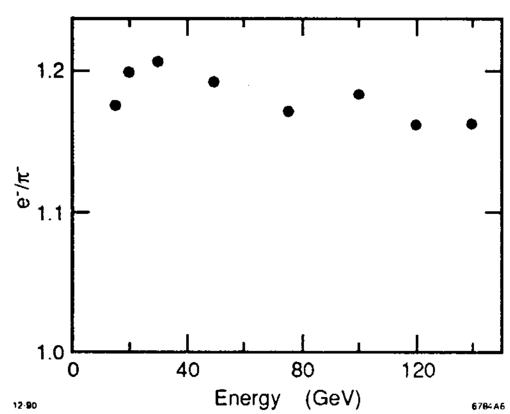

Fig. 5. Ratio of pion to electron response as a function of beam energy. Statistical errors are too small to be seen.

Table 1
Energy and resolution of π-induced interactions.

Beam Energy (GeV)	Number of Events	Mean (NEP)	σ (NEP)	$(\sigma/\text{mean})\sqrt{E_{beam}}$ Resolution
10	7778	36.18	6.63	0.580
15	12842	57.28	8.70	0.588
20	9355	75.14	9.71	0.578
30	12777	115.27	12.74	0.605
50	11187	195.99	17.65	0.637
75	9409	298.19	23.31	0.677
100	3956	402.76	28.32	0.703
120	8099	483.74	33.55	0.760
140	13221	565.02	37.63	0.788

From the measurement of the electron induced showers, the energy of the beam is known and the response is measured directly. From this test, the same ratio for electrons is NEP/GeV = 4.8 ± 0.2.

Comparing the two ratios gives a comparison of the response of the calorimeter to electrons versus that to muons. The ratio of the two (NEP/GeV) ratios is 1.02 ± 0.05, which excludes any large deviations from $e/\mu = 1$.

Longitudinal Shower Development

The longitudinal shower profile is found in this study by summing over all the energy deposited in a plane and averaging.

The results on the longitudinal shower profiles for the electrons is somewhat limited due to the coarse 12.5 cm of iron sampling per phototube. Table 2, however, gives results for the average energy deposited in each plane from the 1984 electron beam. Figure 6 gives a conversion of the electron results to the relative percentage of average energy deposited per plane as a function of the depth in iron of the showers. A clear lengthening of the longitudinal shower profile for electron showers is seen as the beam energy is increased.

For the 1982 pion data, the longitudinal shower profiles are given in table 3 with no attention paid to the location of the shower vertex. Figure 7 gives a plot of the average shower energy deposited per plane as a function of the depth in iron. The figure includes a fit to the profiles using a parameterization by Bock et al.[5] The fit is redone in this report using the same formula:

$$dE = \kappa[\omega s^{-\alpha}\exp(-\beta s) + (1-\omega)t^{-\alpha}\exp(-\delta t)]$$

Table 2
Longitudinal shower profile of e^{-}-induced interactions (NEP).

Beam Energy (GeV)	Planes of 12.5 cm of Iron									
10	31.13	10.01	0.73	0.01						
15	44.78	17.93	1.46	0.08	0.04					
20	57.41	25.86	2.34	0.12						
30	82.38	44.6	4.39	0.24						
50	126.58	86.03	9.91	0.74	0.04					
75	174.34	137.3	17.51	1.3	0.06					
100	212.10	191.80	26.64	2.21	0.13	0.05	0.03	0.02		
100	221.97	191.06	26.49	2.25	0.11	0.03	0.03	0.02	0.01	
100	220.42	190.56	26.42	2.17	0.16	0.06	0.03	0.02		
120	249.53	239.85	35.09	3.23	0.28	0.11	0.09	0.06	0.02	
140	282.37	285.00	42.80	3.98	0.37	0.19	0.09	0.08	0.06	0.05	0.04

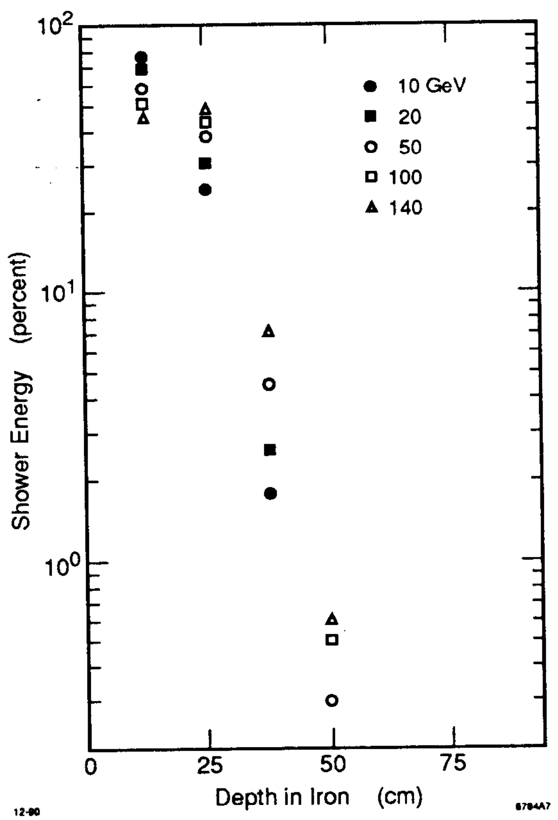

Fig. 6. Relative longitudinal shower energy profile for electron inducedshowers for five different beam energies.

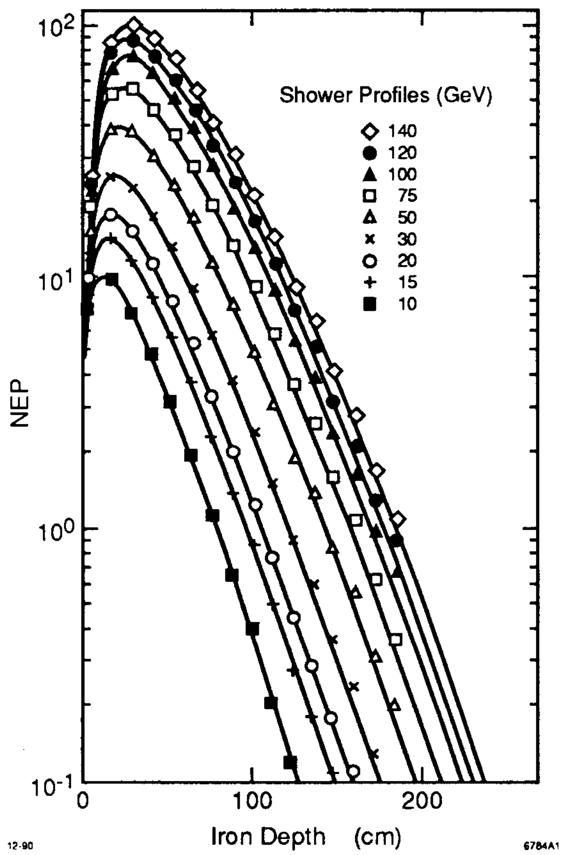

Fig. 7. Longitudinal shower energy profiles for pion induced showers. The fit represents a parameterization given in the text.

Table 3

Longitudinal shower profile of π-induced interactions (NEP).

Beam Energy (GeV)	Planes of 12.5 cm of Iron															
10	7.55	9.81	7.30	4.95	3.20	1.99	1.13	0.66	0.40	0.21	0.12	0.07	0.04	0.02	0	0
15	8.81	14.29	11.71	8.41	5.84	3.81	2.34	1.41	0.87	0.51	0.28	0.18	0.11	0.07	0.04	0.03
20	9.97	17.85	15.31	11.33	8.05	5.44	3.34	2.03	1.27	0.78	0.45	0.29	0.18	0.11	0.06	0.04
30	12.07	25.49	22.92	17.64	13.09	9.16	5.94	3.84	2.44	1.53	0.92	0.61	0.37	0.23	0.13	0.08
50	15.55	38.80	38.42	30.60	23.44	17.38	11.40	7.75	5.05	3.20	1.94	1.40	0.84	0.56	0.31	0.20
75	19.18	53.59	56.33	46.21	36.90	27.88	19.36	13.35	9.07	5.95	3.73	2.63	1.61	1.09	0.64	0.37
100	22.01	66.64	75.07	64.80	51.71	39.87	27.77	18.70	13.01	8.89	5.55	3.92	2.39	1.62	0.97	0.67
120	23.88	77.06	88.71	76.10	61.86	46.69	33.32	23.98	16.63	11.48	7.48	5.31	3.24	2.14	1.31	9.2
140	25.14	85.86	102.24	89.36	74.15	56.59	41.51	30.18	21.37	14.67	9.26	6.39	4.22	2.79	1.71	1.12

The constants "s" and "t" correspond to the radiation length and interaction length in iron (i.e., s = 1.76 cm and t = 19.5 cm). The constant "κ" is a normalization constant that is unimportant in the study of the shapes of these profiles.

A fit using Minuit to the data gives results for the constants generating the curves given in figure 7:

$$\omega = 1.03 - 0.365 \log E \text{ (GeV)}$$

$$\alpha = 0.214 + 0.984 \log E \text{ (GeV)}$$

$$\beta = 0.29$$

$$\delta = 0.978$$

A convolution of these curves with exp (-t) is necessary to take into account the reference to the shower vertex.

Transverse Hadronic Shower Profile

Although only limited precision can be obtained from the 15 cm wide scintillators, some information on the side tails of the shower can be found from the test beam data. Figure 8 shows the fraction of shower energy deposited in the 15 cm wide scintillators as a function of the distance between the scintillator center and the shower center. Only events with an impact point within 1.5 cm scintillator center were selected. As expected, these distributions show that most of the shower energy is deposited in a cone of ~ 15 cm radius with long side tails extending up to 60 cm.

A look at the transverse shower development as a function of the shower depth is given in figure 9. A clear broadening of the shower is observed as the shower develops in the iron.

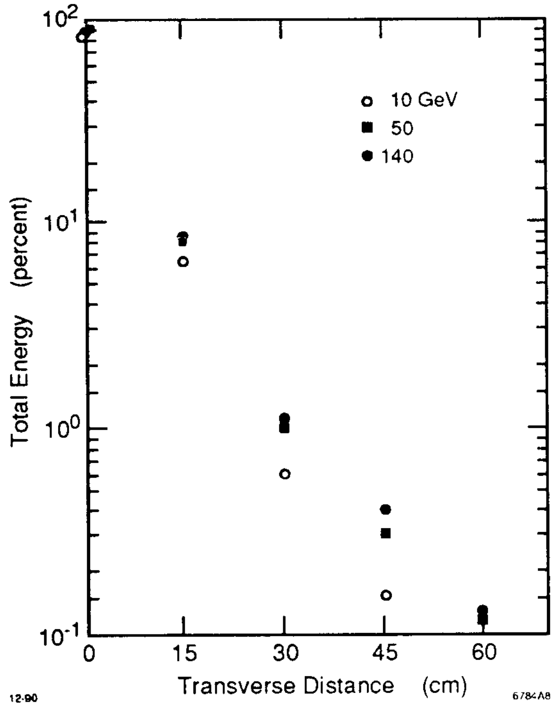

Fig. 8. Transverse shower profiles for pion induced interactions. Results are given in terms of the percentage of shower energy deposited in a scintillator transverse to the shower center. Shower energy is summed longitudinally.

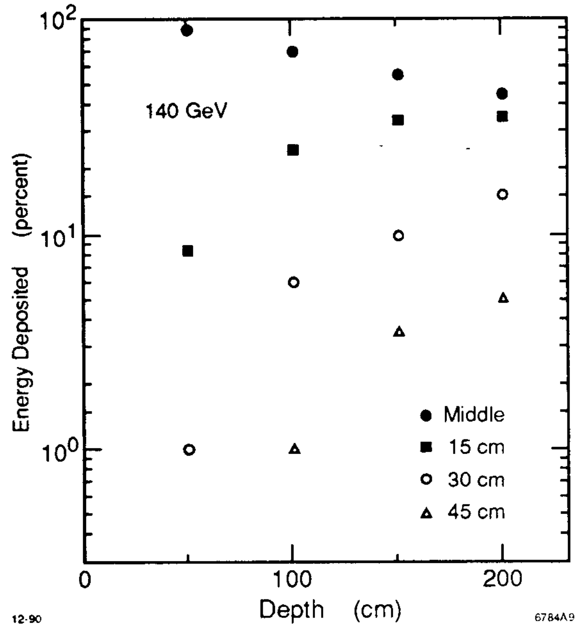

Fig. 9. Percentage of shower energy deposited in scintillators as a function of the depth in the calorimeter for scintillators at different distances transversely with respect to the shower center. For each depth, the total shower energy in a plane is normalized to unity.

Shower Containment

A critical issue for detector construction is shower containment. Figure 10 gives the percentage of shower energy which has leaked out as a function of the calorimeter size. The 100% shower energy containment depth is defined as simply the size of the CDHS calorimeter used in this test. No correction is done for the shower energy which has truly leaked out through the back of the 2 meter calorimeter, but the amount is expected be small. Figure 11 takes the data presented in figure 10 and extracts the length needed to contain 90%, 95%, and 99% of the shower energy as a function of the beam energy. Fits to the three curves are given below:

z(cm) = 70 + 33 log E (GeV) for 99% containment

z(cm) = 53 + 26 log E (GeV) for 95% containment

z(cm) = 41 + 24 log E (GeV) for 90% containment

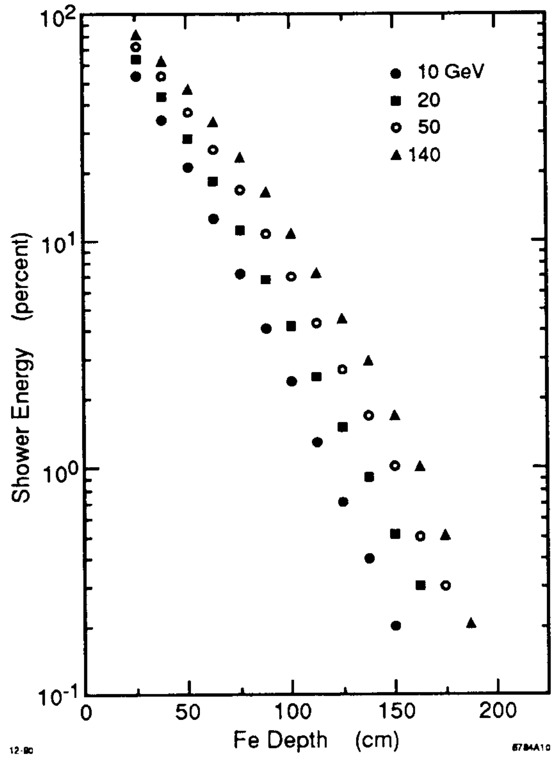

Fig. 10. Percentage of shower energy leakage as a function of calorimeter size for four different pion beam energies.

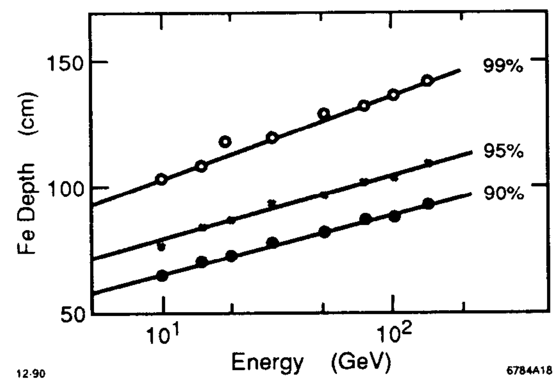

Fig. 11. Calorimeter size needed for given percentage of total shower energy containment as a function of pion beam energy.

Degradation in resolutions as a result of limited detector size often enters into design considerations. Figure 12 presents the resolution as a function of the calorimeter size for four different pion beam energies. The resolution worsens significantly as the containment size is decreased. The resolution worsens by 20% for a calorimeter 120 cm long with 140 GeV pions and 80 cm long for 10 GeV pions.

Shower Correlations

The present data has been used to study correlations between energy deposited between neighboring planes. The results of the study reveal that the shower fluctuations can be understood in terms of a simple model of π^0 and charged hadron production.

The correlation between shower energy deposited in two neighboring planes appear to be uncorrelated when the planes are near the vertex of the shower, but become progressively more correlated when the two neighboring planes are further from the shower vertex. Figure 13 shows the average measured energy deposited in the third plane from the shower vertex as a function of the second plane for three different beam energies. These plots demonstrate only a small linear rise with the energy in the second plane. No correlation would correspond to the same average

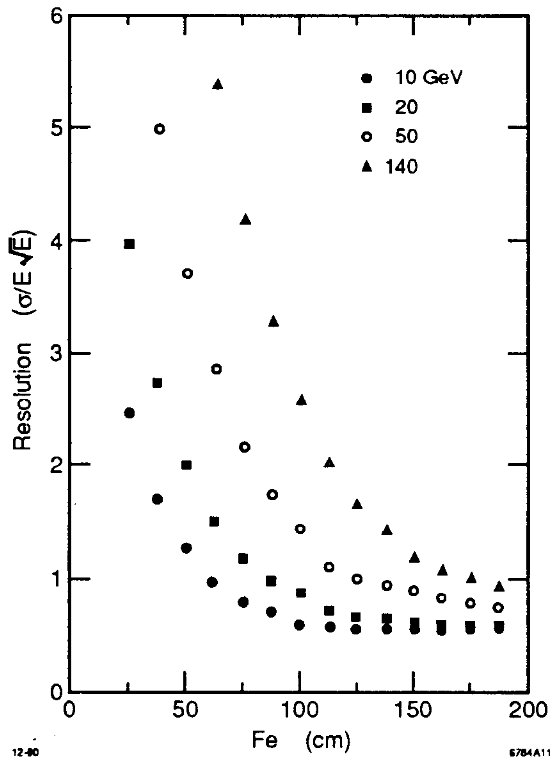

Fig. 12. Resolution as a function of calorimeter size for four different pion beam energies.

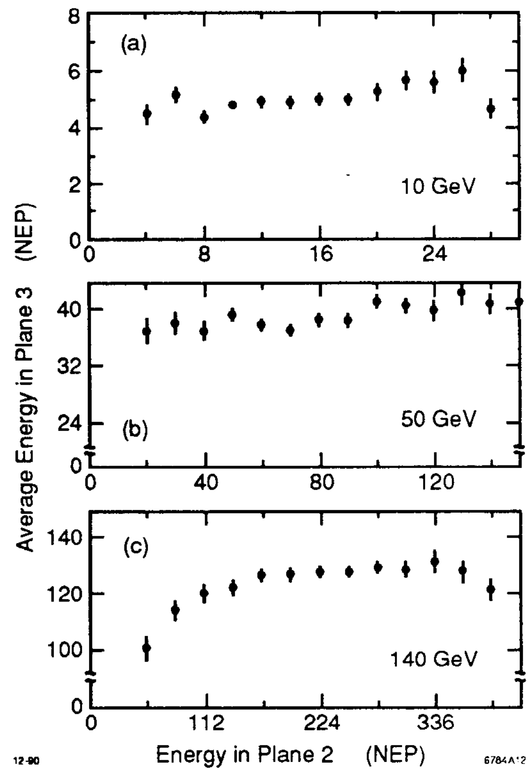

Fig. 13. Average shower energy deposited in the third plane from the vertex as a function of the shower energy deposited in the second plane.

energy deposited in the third plane regardless of the energy deposited in the second plane. Figure 14 shows the same results for the average energy deposited in the fifth plane of the shower versus the energy deposited in the fourth plane. A much steeper rise in the average shower energy, namely a much stronger correlation, is evident.

An explanation for this behavior is that there is a large π^0 production near the shower vertex, which causes large fluctuations in the shower energy per plane, hence little correlation. The π^0 production dies out downstream of the vertex leaving mostly charged hadrons. The charged hadrons typically pass through several planes and deposit a similar energy in neighboring planes, which produces large correlations.

Muon Punch Through

Penetration in absorbers is commonly used to identify muons in large hybrid detectors. A background of deeply penetrating pion induced showers complicates the level of pion to muon discrimination. This section reports on the penetration depth of pion induced showers. Figure 15 shows the probability of finding at least

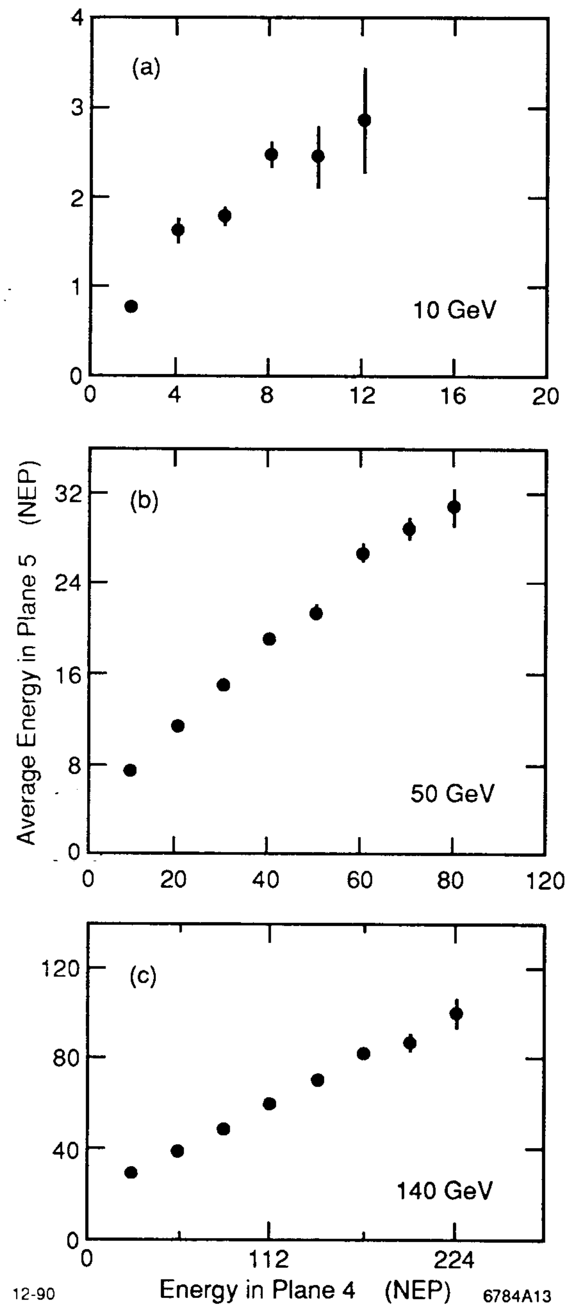

Fig. 14. Average shower energy deposited in the fifth plane from the vertex as a function of the shower energy deposited in the fourth plane.

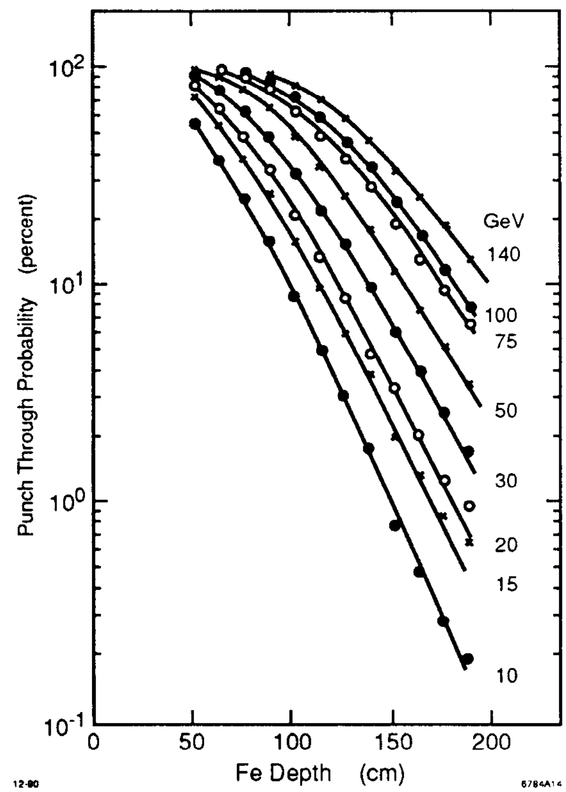

Fig. 15. Probability of a scintillator hit as a function of the calorimeter depth for different pion beam energies.

0.5 NEPs of energy in a plane. Only scintillator located within 22.5 cm of the vertex in the transverse direction were used for this study. In this study, in particular, the transverse segmentation of the scintillators in the CDHS calorimeter plays a crucial role, since noise hits far away from the central particle trajectory are rejected.

The results of this study are sensitive to both noise and inefficiencies in the scintillators. The two effects act in opposite directions to one another in that noise tends to lengthen the track length and scintillator inefficiencies tend to shorten the track length. Some understanding of the level of this cancellation has been done in detail in the measurement of the shower lengths from the study of neutral current interactions.[3] It is from these studies that we choose to use a 0.5 NEP cut. With this energy cut, the track lengthening from noise tends to cancel the track shortening from scintillator inefficiencies. A systematic uncertainty of $\pm$ 10 cm should be included in the results to account for the fact that the two effects may not cancel out.

Dead Plane Studies

In the design of high energy experiments, it is often unavoidable to have some inactive material inside the calorimeter. A simulation of such dead material is easily done by excluding a selected plane (12.5 cm of iron) from the analysis. The response and resolution as a function of the position of the missing plane are given in figures 16 and 17 respectively. Both the resolution and response degrade considerably as long as the dead material is near the vertex of the shower. The poor resolution for dead planes near the beginning of the shower can be seen in the shower distribution illustrated in figure 18.

Conclusions

Calorimeters for the next generation colliders require an understanding of shower development over a large range of energies. Though shower simulation programs are improving and represent a powerful tool for understanding and predicting shower behavior as demonstrated in the present conference, real test beam data with simple detectors still provide the most confidence around which designs can be checked. Even old test beam data such as the present CDHS runs with energies up to 140 GeV still are close to the standard from which simulations and detector designs must be checked.

In summary, the present work presents new results on longitudinal shower profiles with new parameterizations, some details on transverse shower profiles, shower correlations, a measurement of muon punch through and a determination of the response of e-/μ-.

This report represents work done in collaboration with Adam Para and Friedrich Dydak.

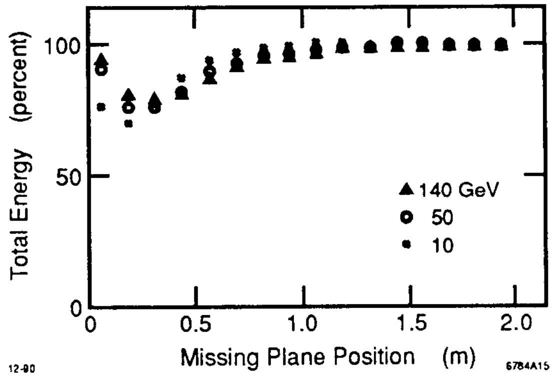

Fig. 16. Percentage of total energy measured as a function of the position of the dead plane.

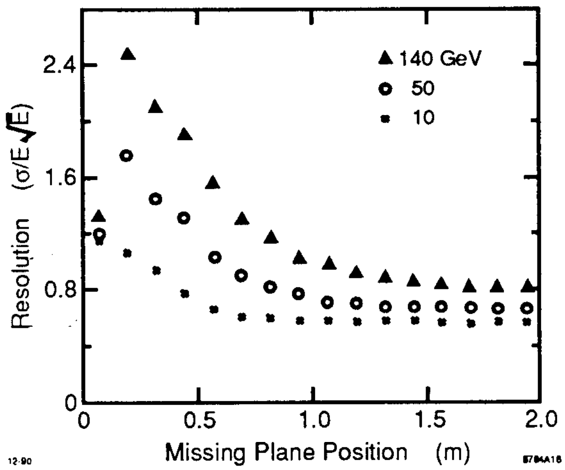

Fig. 17. Resolution measurement as a function of the position of the dead plane.

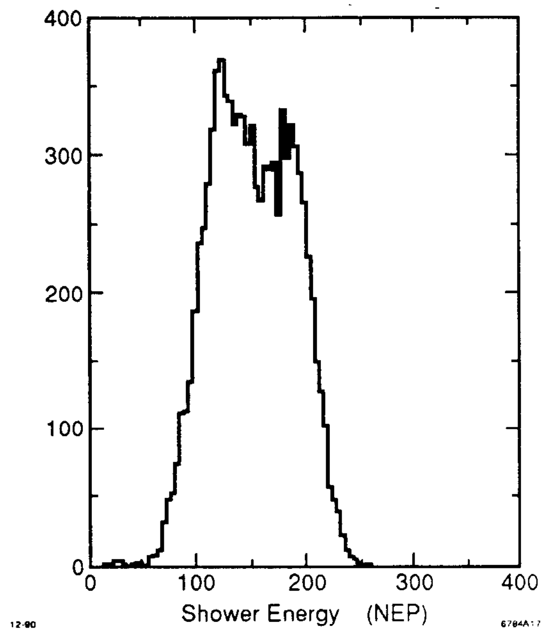

Fig. 18. Shower energy distribution for 50 GeV pions in which the second plane in the calorimeter is dead.

References

1. M. Holder et al., *Nucl. Instrum. Methods,* **151** (1978) 69.
2. D. Hitlin, *Proceedings of the Workshop on Compensated Calorimetry,* (Caltech, 1985).
3. H. Abramowicz et al., *Phys. Rev. Lett.* **57** (1986) 298.
4. C. Richard-Serre, *CERN Yellow Report,* Vol. 71–18, (1971).
5. R. K. Bock et al., Nucl. Instrum. Methods **186** (1981) 533.